Supplementary Material

Catalytic Performance and Reaction Mechanisms of Ethyl Acetate Oxidation over the Au–Pd/TiO2 CatalystsContent

Catalyst characterization procedures:

The actual Au and/or Pd contents in yAu/TiO_2, yPd/TiO_2, and y AuPd$_x$/TiO_2 (x and y are the Au/Pd molar ratio and noble metal content (wt%) of the sample, respectively) were measured using the inductively coupled plasma–atomic emission spectroscopic (ICP–AES) technique on a Thermo Electron IRIS Intrepid ER/S spectrometer. Each sample was dissolved in a mixture of concentrated HCl and HNO_3 aqueous solutions with a volumetric ratio of 3.0 : 1.0 prior to analysis.

The metal dispersion in the samples was measured using an AutoChem II 2920 (Micromeritics) chemical adsorption analyzer. The sample was reduced in a H_2 flow of 30 mL/min at 200 °C for 1 h, purged with a He flow of 30 mL/min for 1 h, and cooled to 40 °C. Then, it was saturated with pulses of CO. The uptake of CO during the chemisorption process was measured by a thermal conductivity detector (TCD) in the chemical adsorption analyzer.

The XRD patterns of the samples were recorded on a Rigaku D/Max RA diffractometer with Cu $K\alpha$ radiation (λ = 0.15418 nm) at 40 kV and 40 mA, and the crystal phases of the samples were identified using the JCPDS database.

To analyze the noble metal particle sizes of the samples, their high-resolution transmission electron microscopic (HRTEM) images were obtained using the JEOL-2010 equipment (operating at 200 kV). High-angle annular dark field–scanning transmission electron microscopic (HAADF–STEM) images and element mappings were acquired on the equipment FEI G2 80-200/Chemi-STEM Cs-corrected transmission electron TEM with a probe corrector. For the preparation of the TEM specimen, we first added the solid powders to a certain volumetric amount of ethanol after ultrasonic dispersion, then dropped the mixture on the carbon foil, and finally obtained the TEM specimen after drying. In the present work, we used the ultra-thin carbon foil (T11032, Beijing XXBR Technology) for the preparation of the TEM specimen and the ultra-thin carbon foil (01824, TED PELLA, INC) for the preparation of the spherical aberration-corrected (Cs) STEM specimen. The particle-size distributions of the samples were estimated by measuring the diameters of 200 particles (according to the HADDF–STEM images) with the origin data processing software.

The BET surface areas of the samples were determined on a Micromeritics ASAP 2020 instrument via N_2 adsorption at −196 °C with the sample being degassed under vacuum at 300 °C for 2 h before measurement, and calculated using the Brunauer–Emmett–Teller (BET) method.

X-ray photoelectron spectroscopy (XPS, Thermo Fisher Scientific ESCALAB 250 Xi spectrometer) was used to measure the O 1s, Pd 3d, Au 4f, and C 1s binding energies (BEs) of surface species, using Mg Kα (hv = 1253.6 eV) as an excitation source. In order to remove the adsorbed water and carbonate species on the surface, the samples were treated in an O_2 flow of 20 mL/min at 250 °C for 1 h and then cooled to RT, followed by transferring the

pretreated samples into the spectrometer in a transparent glove bag filled with helium. The pretreated samples were outgassed in the preparation chamber (10^{-5} Torr) for 0.5 h and then introduced into the analysis chamber (3×10^{-9} Torr) for XPS spectrum recording. All of the peaks were referenced to the BE (284.6 eV) of C 1s for calibration.

Hydrogen temperature-programmed reduction (H_2-TPR) experiments were carried out on a chemical adsorption analyzer (Autochem II 2920, Micromeritics) equipped with a custom-made thermal conductivity detector (TCD). In each measurement, 60 mg of the sample was first pretreated in an O_2 flow of 30 mL/min at 250 °C for 1 h and then cooled to RT for the removal of the adsorbed CO_2 and H_2O. The sample was then subjected to a 10 vol% H_2/Ar (balance) flow of 30 mL/min and heated at a ramp of 10 °C/min from RT to 900 °C. The alteration in H_2 concentration of the effluent was monitored online by the chemical adsorption analyzer. The reduction peak was calibrated against that of the complete reduction of a known standard powered CuO (Aldrich, 99.995%) sample.

Ethyl acetate temperature-programmed surface reaction (Ethyl acetate-TPSR) and temperature-programmed desorption (Ethyl acetate-TPD) experiments were carried out on a chemical adsorption analyzer (Autochem II 2920, Micromeritics) and a mass spectrometer (OmniStar GSD320). Prior to each test, 60 mg of the sample was preheated in an O_2 flow of 30 mL/min at 250 °C for 1 h. After cooling to RT, a (1000 ppm ethyl acetate + N_2 (balance)) mixture flow was passed through the sample. After that, a N_2 flow of 30 mL/min was used to purge the ethyl acetate in the system for 30 min. TPD was carried out in a helium atmosphere after adsorption for 2 h. After the purge process was finished, we heated the sample in a N_2 flow of 30 mL/min from RT to 900 °C, and used a mass spectrometer to monitor the concentration changes of ethyl acetate (m/z = 88), H_2O (m/z = 18), acetaldehyde (m/z = 29, m/z = 42), ethanol (m/z = 31), acetic acid (m/z = 60), propylene oxide (m/z = 58), methyl acetate (m/z = 74) and CO_2 (m/z = 44).

In situ diffuse reflectance Fourier transform infrared spectroscopic (in situ DRIFTS) experiments of the samples were carried out on a Bruker Tensor II spectrometer with a liquid nitrogen-cooling MCT detector. Before the in situ DRIFTS experiment, 30 mg of the sample was loaded on a high-temperature IR cell with ZnSe windows, and preheated in an O_2 flow of 30 mL/min at 250 °C for 1 h. Subsequently, the sample was cooled to RT and purged with a N_2 flow of 30 mL/min for 1 h, and then the background spectrum was recorded at different temperatures. Finally, the sample was kept in a reactant mixture ((1000 ppm ethyl acetate + 20 vol% O_2 + 80 vol% N_2 (balance)) or (1000 ppm ethyl acetate + 50 ppm SO_2 + 20 vol% O_2 + 80 vol% N_2 (balance)) flowing at 10 mL/min, and in situ DRIFTS spectra of the samples in the temperature range of 60−420 °C were recorded by accumulating 32 scans at a spectrum resolution of 4 cm^{-1}.

Catalytic evaluation procedures:

The catalytic activities of the samples were evaluated in a continuous flow, fixed-bed quartz microreactor (i.d. = 6 mm). Because the samples were loaded in the middle of the quartz microreactor, in which the up and down sides of the microreactor were plugged with quartz wool. To avoid the hot spots, 50 mg of the sample (40–60 mesh) was diluted with 0.25 g of quartz sand (40–60 mesh). Prior to the measurement, the sample was pretreated in an O_2 flow of 20 mL/min at 250 °C for 1 h. After being cooled to a given temperature, the ethyl acetate-containing reactant gas mixture was passed through the catalyst bed. The reactant mixture was (1000 ppm ethyl acetate + O_2 + N_2 (balance)), the total flow rate was 33.34 mL/min, with the ethyl acetate/O_2 molar ratio and the space velocity (SV) being 1/400 and ca. 40,000 mL/(g h), respectively. The 1000 ppm ethyl acetate was generated by passing a N_2 flow through a pure ethyl acetate-containing bottle that was chilled in an ice−water isothermal bath at 0 °C. The O_2 and N_2 flow rates were altered to change the SV. In the case of water vapor introduction, 5.0 vol% H_2O was introduced by passing a total reactant flow of 33.34 mL min^{-1} through a water saturator at 33.4 °C. To examine the effect of sulfur dioxide on catalytic activity, we introduced 50 ppm SO_2 to the reaction system in the oxidation of ethyl acetate. Reactants and products were analyzed online on

a gas chromatograph (GC-2010, Shimadzu) equipped with a flame ionization detector (FID) and a TCD, using a stabilwax@-DA column (30 m in length) for VOC separation and a 1/8 in Carboxen 1000 column (3 m in length) for permanent gas separation. The balance of carbon and sulfur throughout the catalytic system was estimated to be 98.5 ± 1.5 % and 99.0 ± 1.0 %, respectively.

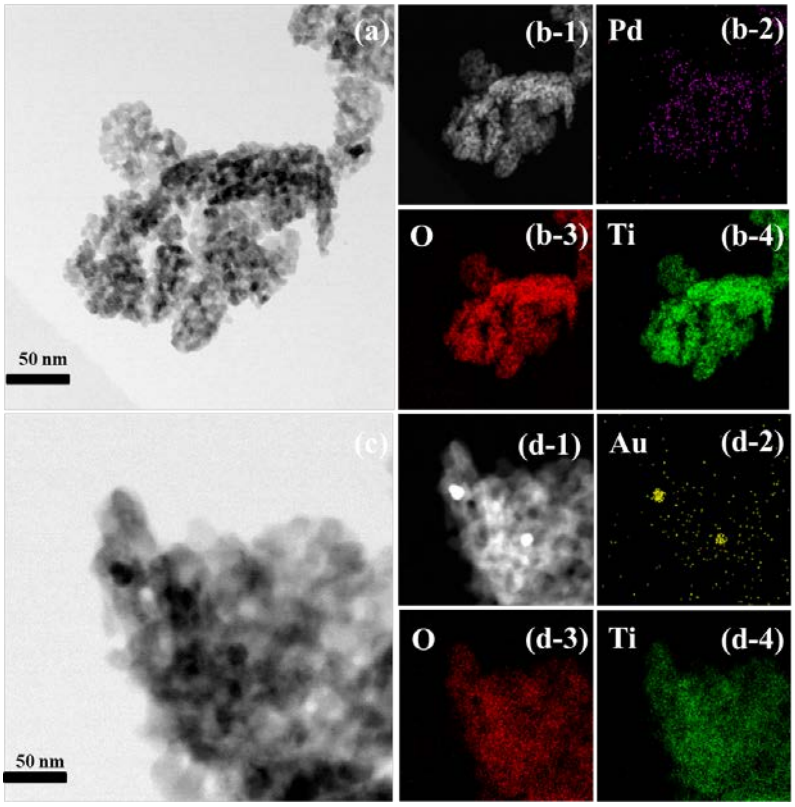

Figure S1. (a, c) TEM images, **(b-1, d-1)** HAADF–STEM images, and **(b-2–b-4, d-2–d-4)** elemental mappings of **(a, b)** 0.33Pd/TiO_2 and **(c, d)** 0.36Au/TiO_2.

Table S1. Comparison on catalytic activities for ethyl acetate oxidation of the 0.37$AuPd_{2.72}$/TiO_2 sample obtained in the present work and the various catalysts reported in the literature.

Catalyst	Ethyl acetate concentration (ppm)	SV (mL/(g h))	$T_{90\%}$ (°C)	Specific reaction rate at 220 °C (μmol/($g_{Noble\ metal}$ s))	Ref.
0.37$AuPd_{2.72}$/TiO_2	1000	40,000	239	67.7	This work
0.63Pd/UiO-66	500	60,000	261	22.7	[40]
0.47Pd/Al_2O_3-pm	1000	50,000	277	55.4	[41]
1Au/CuO	467	600,000	272	25.4	[20]
0.3Pd/SBA-15	970	60,000	238	171.6	[43]
1Ru–5Cu/TiO_2	500	60,000	208	34	[19]
0.84Au/CeO_2	466	600,000	240	92.4	[44]
1Pt/SnO_2	1000	10000	240	8.6	[42]

Table S2. Possible reaction intermediates detected by GC/MS during ethyl acetate oxidation over the 0.34$AuPd_{2.09}$/TiO_2, 0.33Pd/TiO_2, and TiO_2 samples.

Compound	Molecular formula	Structural formula
Nitrogen	N_2	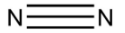
Vinyl formate	HCOOCH = CH_2	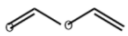
Acetaldehyde	CH_3CHO	

Ethanol	CH_3CH_2OH	
Propylene oxide	C_3H_6O	
Methyl acetate	CH_3COOCH_3	
Propanedioic acid	$HOOCCH_2COOH$	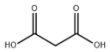
4-Hydroxy-2-butanone	$CH_3COCH_2CH_2OH$	
(3-methyloxiran-2-yl)methanol	$C_4H_8O_2$	
Ethyl acetate	$CH_3COOCH_2CH_3$	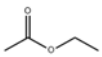
Acetic acid	CH_3COOH	

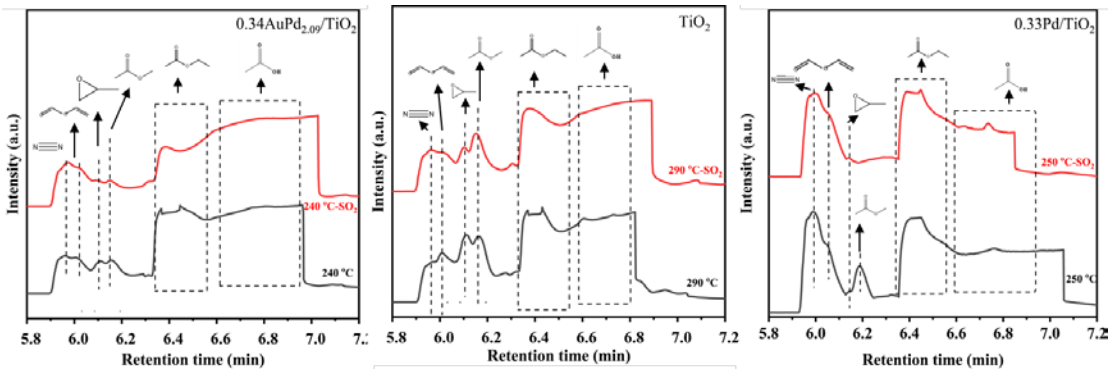

Figure S2. Possible reaction intermediates detected during the ethyl acetate oxidation process at $T_{90\%}$ and SV = 40,000 mL/(g h) over the 0.34AuPd$_{2.09}$/TiO$_2$, TiO$_2$, and 0.33Pd/TiO$_2$ samples in the presence or absence of SO$_2$.

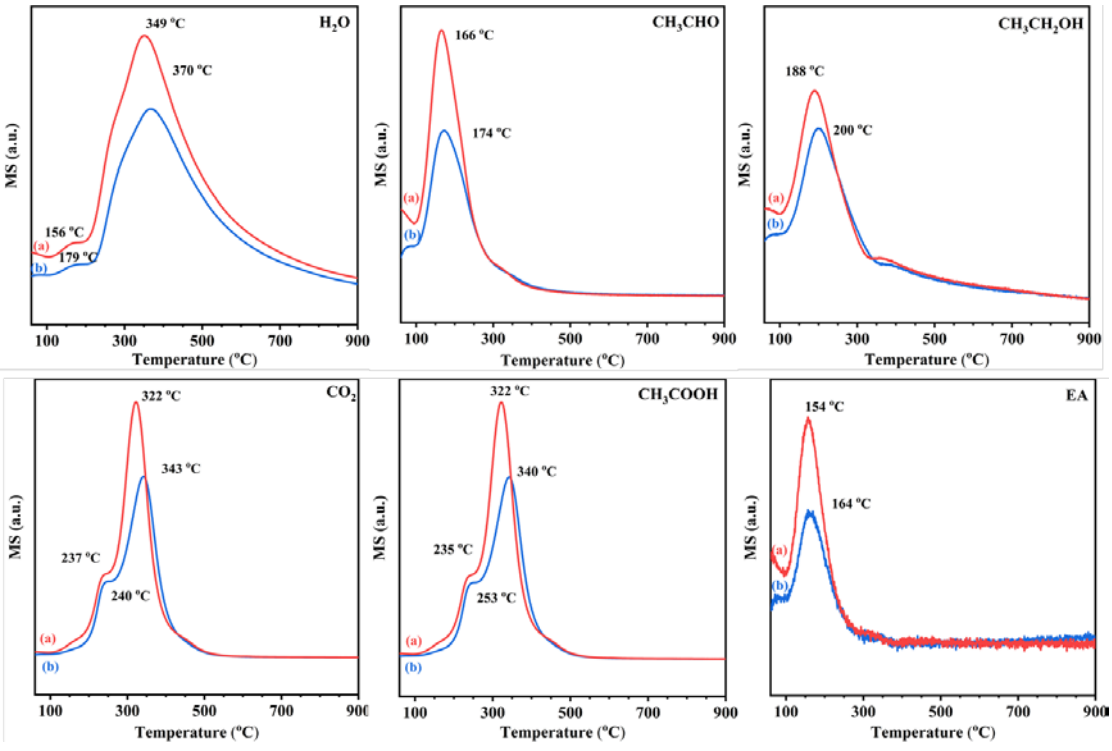

Figure S3. TPSR profiles of **(a)** 0.34AuPd$_{2.09}$/TiO$_2$ and **(b)** 0.33Pd/TiO$_2$ for ethyl acetate oxidation.

References

19. Liu, X.L.; Han, Q.Z.; Shi, W.B.; Zhang, C.; Li, E.W.; Zhu, T.Y. Catalytic oxidation of ethyl acetate over Ru–Cu bimetallic catalysts: Further insights into reaction mechanism via in situ FTIR and DFT studies. J. Catal. ***2019****, 369, 482–492.*

20. Carabineiro, S. A. C.; Chen, X.; Martynyuk, O.; Bogdanchikova, N.; Avalos-Borja, M.; Pestryakov, A.; Tavares, P. B.; Órfão, J. J. M.; Pereira, M. F. R.; Figueiredo, J. L. Gold supported on metal oxides for volatile organic compounds total oxidation. *Catal. Today* **2015**, *244*, 103–114.

48. Li, J.T.; Xu, Z.L.; Wang, T.; Xie, X.W.; Li, D.D.; Wang, J.G.; Huang, H.B.; Ao, Z.M., A Versatile Route to Fabricate Metal/UiO-66 (Metal = Pt, Pd, Ru) with High Activity and Stability for the Catalytic Oxidation of Various Volatile Organic Compounds. *Chem. Eng. J.* **2022**, *448*, 136900.

49. Ma, M.D.; Yang, R.; He, C.; Jiang, Z.Y.; Shi, J. W.; Albilali, R.; Fayaz, K.; Liu, B.J., Pd-based catalysts promoted by hierarchical porous Al_2O_3 and ZnO microsphere supports/coatings for ethyl acetate highly active and stable destruction. *J. Hazard. Mater.* **2021**, *401*, 123281.

50. Kamiuchi, N.; Mitsui, T.; Yamaguchi, N.; Muroyama, H.; Matsui, T.; Kikuchi, R.; Eguchi, K., Activation of Pt/SnO_2 catalyst for catalytic oxidation of volatile organic compounds. *Catal. Today* **2010**, *157*, 415−419.

51. He, C.; Yue, L.; Zhang, X.Y.; Li, P.; Dou, B.J.; Ma, C.Y.; Hao, Z.P., Deep catalytic oxidation of benzene, toluene, ethyl acetate over Pd/SBA-15 catalyst: reaction behaviors and kinetics. *Asia-Pac. J. Chem. Eng.* **2012**, *7*, 705−715.

52. Bastos, S. S. T.; Carabineiro, S. A. C.; Órfão, J. J. M.; Pereira, M. F. R.; Delgado, J. J.; Figueiredo, J. L., Total oxidation of ethyl acetate, ethanol and toluene catalyzed by exotemplated manganese and cerium oxides loaded with gold. *Catal. Today* **2012**, *180*, 148−154.